Novel scanning method for distortion-free BOTDA measurements

Alejandro Dominguez-Lopez,[1,*] Zhisheng Yang,[2,3] Marcelo A. Soto,[2] Xabier Angulo-Vinuesa,[1] Sonia Martin-Lopez,[1] Luc Thevenaz,[2] and Miguel Gonzalez-Herraez[1]

[1]*Dept. of Electronics, University of Alcala, Polytechnic School, 28805 Alcala de Henares, Spain*
[2]*EPFL Swiss Federal Institute of Technology, Institute of Electrical Engineering, SCI-STI-LT Station 11, CH-1015 Lausanne, Switzerland*
[3]*Permanent address: State Key Laboratory of Information Photonics & Optical Communications, Beijing University of Posts and Telecommunications, Beijing 100876, China*
[*]*alejandro.dominguezl@uah.es*

Abstract: Systematic errors induced by distortions in the pump pulse of conventional Brillouin distributed fiber sensors are thoroughly investigated. Experimental results, supported by a theoretical analysis, demonstrate that the two probe sidebands in standard Brillouin optical time-domain analyzers provide a non-zero net gain on the pump pulse, inducing severe distortions of the pump when scanning the pump-probe frequency offset, especially at high probe power levels. Compared to the impact of non-local effects reported in the state-of-the-art, measurements here indicate that for probe powers in the mW range (below the onset of amplified spontaneous Brillouin scattering), the obtained gain and loss spectra show two strong side-lobes that lead to significant strain/temperature errors. This phenomenon is not related to the well-known spectral hole burning resulting from pump depletion, but it is strictly related to the temporal and spectral distortions that the pump pulse experiences when scanning the Brillouin gain/loss spectrum. As a solution to this problem, a novel scanning scheme for Brillouin sensing is proposed. The method relies on a fixed frequency separation between the two probe sidebands, so that a flat zero net gain is achieved on the pump pulse when scanning the pump-probe frequency offset. The proposed technique is experimentally validated, demonstrating its ability to completely cancel out non-local effects up to a probe power ultimately limited by the onset of amplified spontaneous Brillouin scattering. The method allows for one order of magnitude improvement in the figure-of-merit of optimized long-range Brillouin distributed fiber sensors, enabling measurements along a 100 km-long sensing fiber with 2 m spatial resolution and with no need of added features for performance enhancement.

OCIS codes: (060.2370) Fiber optics sensors; (290.5900) Scattering, stimulated Brillouin; (060.4370) Nonlinear optics, fibers.

References and links

1. T. Horiguchi, K. Shimizu, T. Kurashima, M. Tateda, and Y. Koyamada, "Development of a distributed sensing technique using Brillouin scattering," J. Lightwave Technol. **13**(7), 1296–1302 (1995).
2. M. Nikles, L. Thévenaz, and P. A. Robert, "Brillouin gain spectrum characterization in single-mode optical fibers," J. Lightwave Technol. **15**(10), 1842–1851 (1997).
3. E. Geinitz, S. Jetschke, U. Röpke, S. Schröter, R. Willsch, and H. Bartelt, "The influence of pulse amplification on distributed fibre-optic Brillouin sensing and a method to compensate for systematic errors," Meas. Sci. Technol. **10**(2), 112–116 (1999).
4. A. Minardo, R. Bernini, L. Zeni, L. Thevenaz, and F. Briffod, "A re-construction technique for long-range stimulated Brillouin scattering distributed fiber-optic sensors: Experimental results," Meas. Sci. Technol. **16**(4), 900–908 (2005).

#259757 Received 19 Feb 2016; revised 22 Apr 2016; accepted 24 Apr 2016; published 2 May 2016

5. L. Thévenaz, S. F. Mafang, and J. Lin, "Effect of pulse depletion in a Brillouin optical time-domain analysis system," Opt. Express **21**(12), 14017–14035 (2013).
6. M. A. Soto and L. Thévenaz, "Modeling and evaluating the performance of Brillouin distributed optical fiber sensors," Opt. Express **21**(25), 31347–31366 (2013).
7. Z. Yang, X. Hong, J. Wu, H. Guo, and J. Lin, "Theoretical and experimental investigation of an 82-km-long distributed Brillouin fiber sensor based on double sideband modulated probe wave," Opt. Eng. **51**(12), 124402 (2012).
8. A. Minardo, R. Bernini, and L. Zeni, "A simple technique for reducing pump depletion in long-range distributed Brillouin fiber sensors," IEEE Sens. J. **9**(6), 633–634 (2009).
9. A. Domínguez-López, X. Angulo-Vinuesa, A. López-Gil, S. Martín-López, and M. González-Herráez, "Non-local effects in dual-probe-sideband Brillouin optical time domain analysis," Opt. Express **23**(8), 10341–10352 (2015).
10. R. Ruiz-Lombera, J. Urricelqui, M. Sagues, J. Mirapeix, J. M. López-Higuera, and A. Loayssa, "Overcoming nonlocal effects and Brillouin threshold limitations in Brillouin optical time-domain sensors," IEEE Photonics J. **7**(6), 1–9 (2015).
11. S. Diaz, S. Foaleng Mafang, M. Lopez-Amo, and L. Thevenaz, "A high-performance optical time-domain Brillouin distributed fiber sensor," IEEE Sens. J. **8**(7), 1268–1272 (2008).
12. M. A. Soto, G. Bolognini, F. Di Pasquale, and L. Thévenaz, "Simplex-coded BOTDA fiber sensor with 1 m spatial resolution over a 50 km range," Opt. Lett. **35**(2), 259–261 (2010).
13. M. A. Soto, G. Bolognini, F. Di Pasquale, and L. Thévenaz, "Long-range Brillouin optical time-domain analysis sensor employing pulse coding techniques," Meas. Sci. Technol. **21**(9), 094024 (2010).
14. S. Martin-Lopez, M. Alcon-Camas, F. Rodriguez, P. Corredera, J. D. Ania-Castañon, L. Thévenaz, and M. Gonzalez-Herraez, "Brillouin optical time-domain analysis assisted by second-order Raman amplification," Opt. Express **18**(18), 18769–18778 (2010).
15. F. Rodriguez-Barrios, S. Martin-Lopez, A. Carrasco-Sanz, P. Corredera, J. D. Ania-Castanon, L. Thévenaz, and M. Gonzalez-Herraez, "Distributed Brillouin fiber sensor assisted by first-order Raman amplification," J. Lightwave Technol. **28**(15), 2162–2172 (2010).
16. M. A. Soto, J. A. Ramírez, and L. Thévenaz, "Intensifying Brillouin distributed fibre sensors using image processing," Proc. SPIE **9634**, 96342D (2015).
17. M. A. Soto, J. A. Ramírez, and L. Thévenaz, "Intensifying the response of distributed optical fibre sensors using 2D and 3D image restoration," Nat. Commun. **7**, 10870 (2016).
18. M. A. Soto, G. Bolognini, and F. Di Pasquale, "Simplex-coded BOTDA sensor over 120 km SMF with 1 m spatial resolution assisted by optimized bidirectional Raman amplification," IEEE Photonics Technol. Lett. **24**(20), 1823–1826 (2012).
19. M. A. Soto, X. Angulo-Vinuesa, S. Martin-Lopez, S.-H. Chin, J. D. Ania-Castanon, P. Corredera, E. Rochat, M. Gonzalez-Herraez, and L. Thévenaz, "Extending the real remoteness of long-range Brillouin optical time-domain fiber analyzers," J. Lightwave Technol. **32**(1), 152–162 (2014).
20. J. Urricelqui, M. A. Soto, and L. Thévenaz, "Sources of noise in Brillouin optical time-domain analyzers," Proc. SPIE **9634**, 96342D (2015).

1. Introduction

Distributed optical fiber sensors based on Brillouin optical time-domain analysis (BOTDA) [1] have been widely employed for various physical sensing applications such as temperature and strain measurements. The basic interrogation scheme consists of a pump pulse that interacts with a counter-propagating continuous wave probe through stimulated Brillouin scattering (SBS) [1]. When the frequency offset of the pump and probe wave falls within the Brillouin gain/loss spectrum (BGS/BLS), the probe is amplified/depleted by the pump pulse during the interaction process. As the central frequency of the gain/loss spectrum depends linearly on strain and temperature, any change in these quantities can be detected by measuring the spectral shift of the peak Brillouin gain/loss frequency [1,2]. By scanning the frequency difference between the pump pulse and the probe, the Brillouin frequency shift (BFS) at each position along the fiber can be found. This technique works under the assumption that the pump power only experiences the fiber attenuation as it propagates along the sensing fiber. However, during propagation the pump pulse continuously transfers energy to the probe or receives energy from the probe, depending on whether the frequency of the pump pulse is higher or lower than that of the probe. When the accumulated energy transfer is very high (non-negligible compared to the pulse energy), non-local effects are induced [3,4], shifting the local BGS and giving rise to errors in the estimated BFS profile [5]. Either long-range sensors or short-range systems based on a high-power probe are affected by these non-local effects. This detrimental problem highly limits the allowable probe power that can be

#259757 Received 19 Feb 2016; revised 22 Apr 2016; accepted 24 Apr 2016; published 2 May 2016

launched into the sensing fiber, imposing significant constraints to the signal-to-noise ratio (SNR) and sensor performance [6].

To partially overcome this problem, the use of a double-sideband (DSB) probe [2] has been so far considered as the most reliable and simple method to mitigate pump depletion and non-local effects [2,5,7,8], allowing, in principle, a maximum probe power determined by the onset of amplified spontaneous Brillouin scattering (ASpBS). However, it has been recently reported [9] that the DSB probe technique is still affected by detrimental non-local effects, which result from the asymmetric nature of the frequency scanning process required by the method. Reference [9] actually shows that the spectral shape of the pump pulse can be significantly distorted as a consequence of the non-zero and asymmetric net Brillouin gain generated by the two probe sidebands when scanning the modulation frequency. The spectral distortion manifests as a spectrally-asymmetric growth of the pump pulse power depending on the exact detuning from the BFS frequency. Such a spectral distortion is directly related to the probe power and the sensing fiber length, thus preventing the probe wave from reaching the power of ASpBS threshold. Very recently, another interesting work [10] has studied the distortion induced to the pump due to a dual-probe scheme in BOTDA and a smart solution is proposed to solve it by synchronously dithering the probe frequency, at the expense of an enlarged frequency scanning range, accordingly. A non-distorting BOTDA system is demonstrated over a total distance of 50 km, featuring 5 m of spatial resolution using a high probe power (8 dBm/sideband).

An important aspect of the reported phenomenon is that it affects not only standard BOTDA configurations [6–9,11], but also any other advanced technique making use of the DSB/SSB probe scheme [12–19]. Actually, methods such as pulse coding [12,13], Raman distributed amplification [14,15], image processing [16,17], and some combinations of them [18,19] have allowed a significant boost in SNR and sensor performance; however, their capability to enable implementations with very high figure-of-merit [6] has been compromised by the use of low probe power levels, thus preventing those advanced techniques from performing at their maximum potential. Providing a solution to pump depletion issues, which could also enable the use of advanced methods, would be a significant step forward to enhance the performance of BOTDA sensors.

This paper presents a thorough analysis of the temporal and spectral distortions that the pump pulse experiences in DSB schemes, along with their impact on the BOTDA sensor performance when using high probe powers (i.e. close to the ultimate limit imposed by the ASpBS threshold), complementing preliminary results reported in [9,10]. It particularly follows our previous work [9], where spectral distortions were observed with probe power levels ranging up to −3 dBm/sideband. Here it is shown that the impact of the pump pulse distortion becomes observable at a probe power of about −5 dBm/sideband, however, when the probe power increases and approaches 0 dBm/sideband, an asymmetric push-pull effect in the pulse spectrum occurs as a consequence of the asymmetric Brillouin gain and loss affecting the pulse. Compared to the previously reported spectral distortions [9], in this paper it is demonstrated that such a detrimental effect on the pulse spectrum leads also to a serious temporal broadening of the pulse, giving rise to a deleterious effect on the system resolution. Furthermore, it is here shown that when the probe power goes beyond the mW range (e.g. higher than about 0 dBm), an unexpectedly huge amplification of the pump pulse occurs, leading to intolerable spectral distortions that impair considerably the sensor response. As a solution to this problem, a novel scheme for scanning the pump-probe frequency offset in BOTDA sensors is here proposed. Instead of symmetrically scanning the frequency of the two probe sidebands away or towards the pump pulse frequency, the proposed method fixes the spectral separation between the probe sidebands, and sweeps them together to acquire the BGS information. This way, a zero net Brillouin gain on the pump can be obtained during the entire scanning process, regardless the pump-probe frequency offset. Experimental results show that the proposed method can successfully overcome the problems induced by non-local

#259757 Received 19 Feb 2016; revised 22 Apr 2016; accepted 24 Apr 2016; published 2 May 2016

effects, allowing the power of each probe sideband to be increased from –5 dBm up to the ultimate limit of 7 dBm imposed by the threshold of ASpBS. This demonstrates a 12 dB probe power enhancement, which, in thermal-noise-limited BOTDA sensors can be directly translated to an equivalent SNR improvement [6,20]. Furthermore, the technique can be straightforwardly combined with advanced methods for further SNR enhancement.

2. Spectral and temporal pump distortion in conventional DSB schemes

Recently the evidence of a series of non-local effects in DSB-based BOTDA schemes arising from probe powers way below the ASpBS threshold has been reported in [9,10]. Such previous work focused on the study of the spectral evolution of the pump pulse using moderate probe powers (up to about –3 dBm/sideband) and long input pulses (50 ns pulse width). It has been shown that the pulse spectrum in that case experiences distortion and a spectral up or down-shifting when sweeping the probe wave modulation frequency in the conventional scanning process of BOTDA sensors. This spectral distortion has a much greater detrimental effect on the probe wave at the anti-Stokes frequency (Brillouin loss), which manifests as a substantial broadening of the measured loss spectrum and the appearance of two asymmetric side-lobes around the BFS. However, in the case of measuring the probe wave at the Stokes frequency (Brillouin gain), the pump spectral distortion is small for the probe power range reported in [9], and is mostly visible as a narrowing of the gain spectral shape.

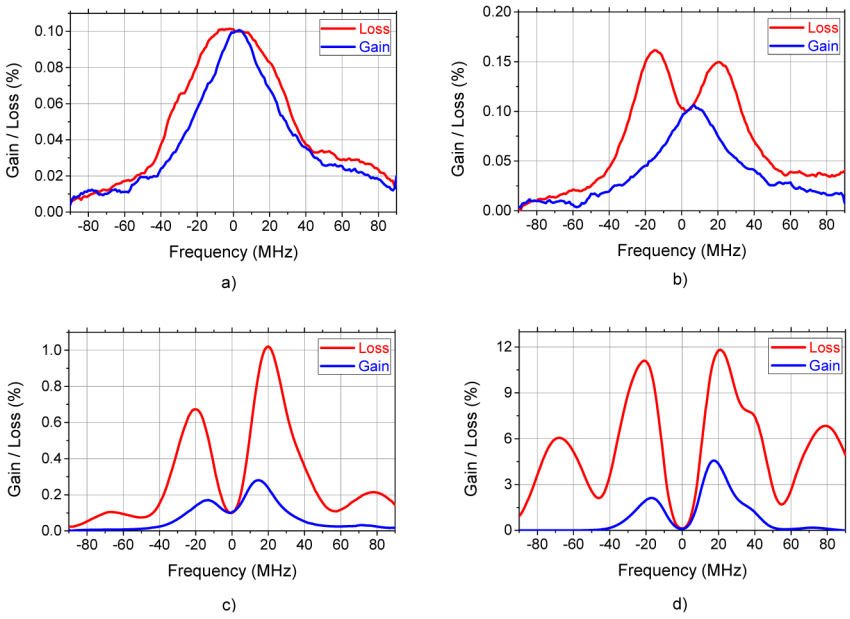

Fig. 1. Measured BGS/BLS at the end of a 50 km optical fiber using a conventional BOTDA sensor with 2 m spatial resolution, for different probe power levels: (a) –5 dBm/sideband; (b) –2 dBm/sideband; (c) 1 dBm/sideband; and (d) 4 dBm/sideband. Red curve: BLS; blue curve: BGS. Spectral distortions originate from the asymmetric Brillouin gain and loss process affecting the pump pulse while scanning the pump-probe frequency offset around the BFS.

In this section, those findings are complemented and more deeply investigated in a much larger probe power range, including also an investigation on the temporal distortion of the pulse shape for different pulse lengths and different frequency detuning. For this analysis, a conventional BOTDA scheme based on a two-sideband probe has been used [7,8,11]. Scanning the pump-probe frequency offset around the BFS of a 50 km-long single-mode fiber, and using a 20 ns pulse for 2 m spatial resolution, the BGS and BLS have been

#259757 Received 19 Feb 2016; revised 22 Apr 2016; accepted 24 Apr 2016; published 2 May 2016

measured for different probe power levels (a pump power of 80 mW has been used in all measurements). Figure 1 shows the measured BGS (blue curves) and BLS (red curves) obtained at the end of the sensing fiber (at 50 km distance), for a probe power per sideband of (a) –5 dBm, (b) –2 dBm, (c) + 1 dBm and (d) + 4 dBm. Experimental results point out that, for –5 dBm probe power, although there appear minimum distortions in the measured spectra, such distortions are negligible, while with the use of moderate probe powers the spectral distortion becomes evident. Actually, the narrowing effect observed in the gain spectrum and the broadening measured in the loss spectrum for –5 dBm and –2 dBm [see Figs. 1(a)-1(b)] match the behavior reported in [9]. However, a novel and unexpected behavior could be found with powers reaching and exceeding the mW range: for such a high probe power (e.g. more than about 0 dBm), both the BGS and BLS show a peak splitting around the BFS.

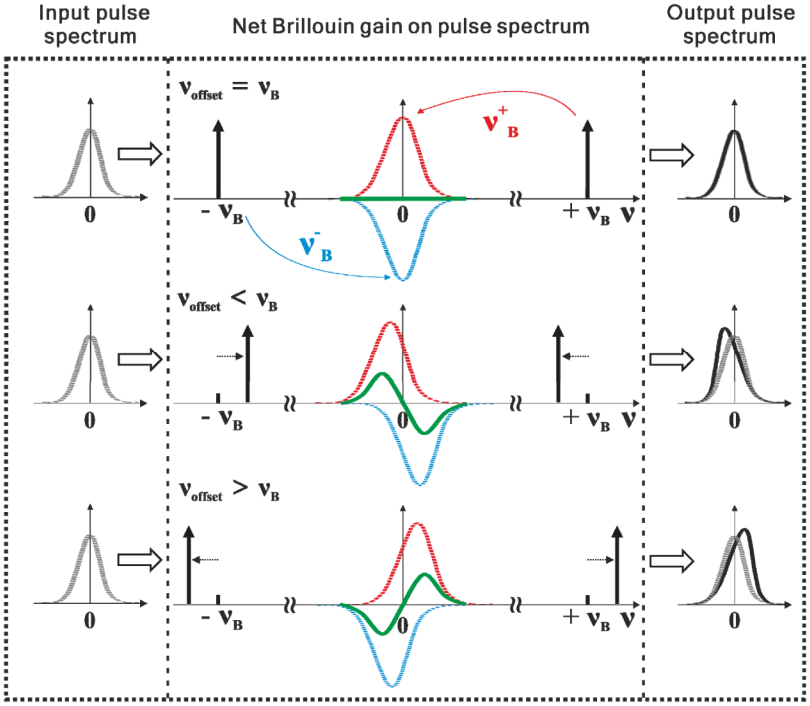

Fig. 2. Net Brillouin gain affecting the pump pulse while scanning the pump-probe frequency offset (ν_{offset}) symmetrically around the pulse spectrum in a conventional BOTDA scheme. Grey dotted lines: input pulse spectrum; red dotted lines: Brillouin gain spectrum generated by the upper-frequency probe sideband; blue dotted lines: Brillouin loss spectrum generated by the lower-frequency probe sideband; green solid lines: net Brillouin gain spectrum experienced by the pulse; black solid line: output pulse spectrum after SBS interaction.

In order to have a better insight into the process and to provide an explanation of the spectral distortions shown in Fig. 1, Figs. 2 and 3 show schematic descriptions of the pump-probe Brillouin interactions occurring in a standard DSB-based scanning method. By sweeping the frequency of the two sidebands in the traditional way [2,7–9,11], as shown in Fig. 2, the pump pulse spectrum is subject to an uneven spectral compensation of the gain-loss probe spectra in case of detuning. The pulse spectrum turns out to be then asymmetrically distorted and downshifted or upshifted as the pulse propagates along the sensing fiber, depending on whether the scanned pump-probe frequency offset (ν_{offset}) is higher or lower than the dominant BFS of the fiber [9]. This detrimental effect comes from the non-zero net gain (indicated by green lines in Fig. 2) that combines Brillouin gain (red curves) and loss (blue curves) spectra generated by the upper and lower probe sidebands, respectively. This

#259757 Received 19 Feb 2016; revised 22 Apr 2016; accepted 24 Apr 2016; published 2 May 2016

pulse distortion cumulates along the sensing fiber, and depending on the probe power level, two probe power regimes could be defined to better classify the non-local phenomena affecting the overall SBS interaction.

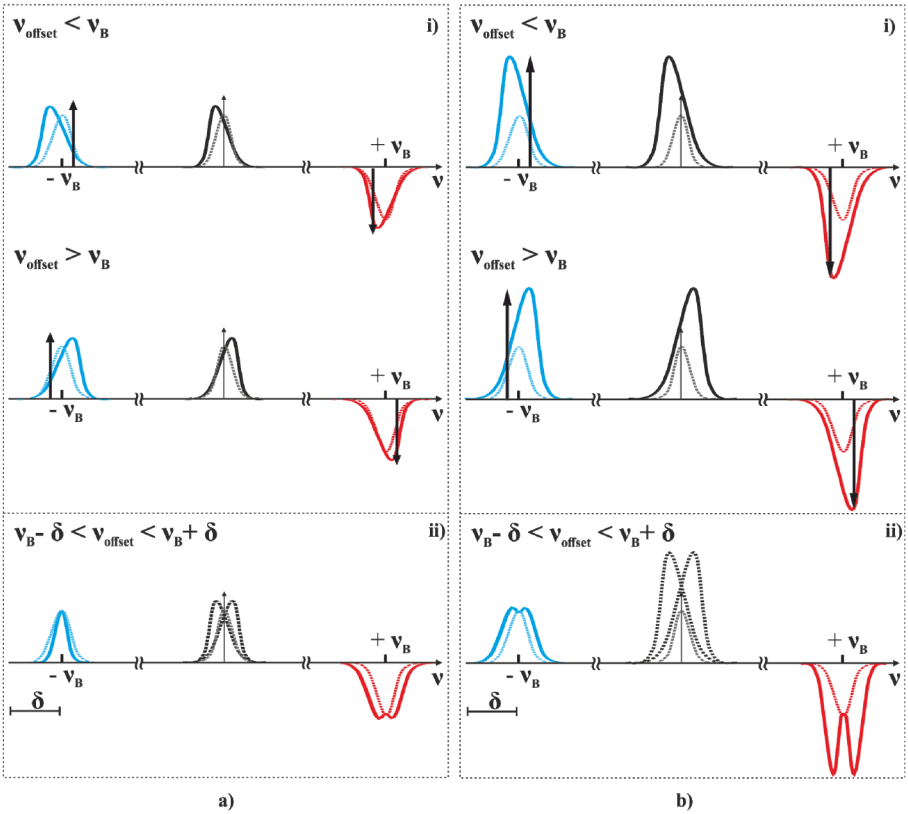

Fig. 3. Illustration of the SBS interaction between a non-symmetric pulse spectrum and the Brillouin gain and loss curves while scanning the pump-probe frequency offset (ν_{offset}) around the BFS, for different probe powers: (a) low-to-medium power regime; (b) high power regime. Dotted lines represent the original undistorted pulse (black), gain (blue) and loss (red) spectra. (i) Individual gain and loss processes at given scanning frequencies, and (ii) spectral shape resulting from the complete measurement process in a conventional BOTDA sensor.

The first regime occurs at low-to-medium power levels, i.e. for probe powers below the mW range, and leads to the distortions shown in Figs. 1(a)-1(b). As described in Fig. 3(a), while scanning the pump-probe frequency offset around the BFS, the measured spectra turn out to be distorted. Although the peak pump power is only mildly affected with this low-to-medium probe power, the Brillouin loss spectrum progressively broadens out showing two peaks around the BFS when augmenting the probe power, while the Brillouin gain spectrum narrows, showing only a minor distortion.

The second regime occurs at high probe powers, ranging from about 0 dBm up to the threshold of ASpBS (about + 7 dBm). In this case, the pump-probe interaction is similar to the previous case; however, the net asymmetric Brillouin gain (see green line in Fig. 2) amplifying and distorting the pump pulses highly cumulate along the fiber, increasing with a strong nonlinear dependency on the probe power. This leads to BGS and BLS having two strong peaks around the central BFS [see Fig. 3(b)], as demonstrated in the measurements previously shown in Figs. 1(c)-1(d). An interesting feature is that for such high-power regime, the induced detrimental effects grow exponentially with the probe power, which can dramatically worsen the system performance. This is a completely different behavior when

#259757 Received 19 Feb 2016; revised 22 Apr 2016; accepted 24 Apr 2016; published 2 May 2016

compared to results reported in [9], and actually has a more detrimental impact on the measurements since the obtained spectrum splits into side-lobes, independently of the measured processes (i.e. it occurs for both the BGS and BLS).

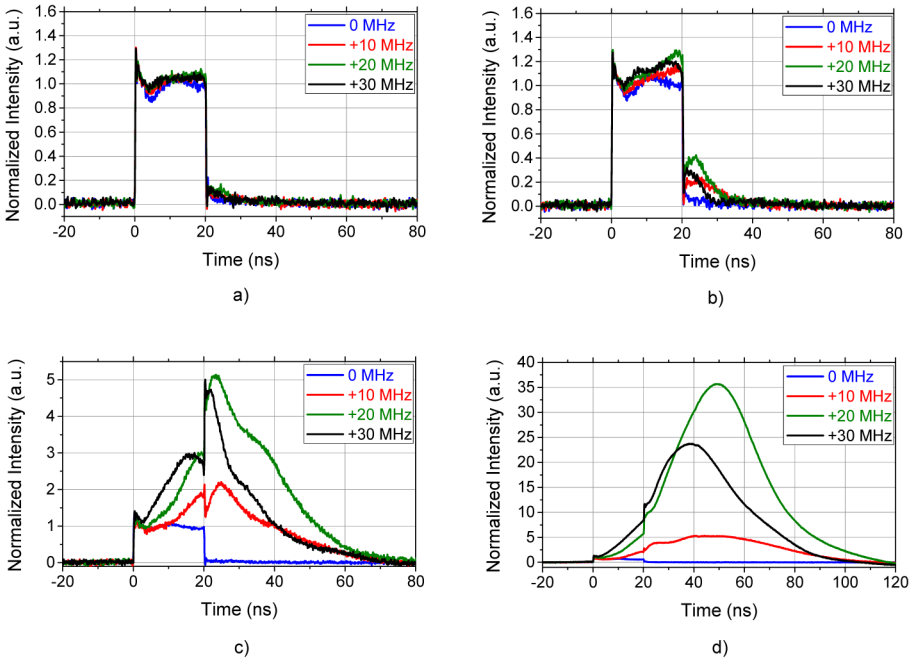

Fig. 4. Temporal distortion of a 20 ns pump pulse, for different pump-probe positive frequency detuning and using probe powers of (a) –5 dBm/sideband; (b) –2 dBm/sideband; (c) 1 dBm/sideband; and (d) 4 dBm/sideband.

In addition to the above-reported spectral distortions, the pump pulses also experience significant temporal deformation after interacting with the two-sideband probe through long sensing fibers. Figure 4 shows a set of measurements analyzing the deformation of the pulse temporal shape at the output of the 50 km sensing fiber for different probe powers, when varying the probe wave modulation frequency around the BFS. Actually, when the probe wave modulation frequency matches the BFS of the fiber, gain and loss induced by the sidebands on the pump pulse compensate, and there is no distortion, broadening or amplification on the pump pulse shape. However, as shown in Fig. 4, when the probe wave modulation frequency is detuned from the BFS of the fiber (positive detuning), the asymmetric non-zero net gain affecting the pump pulses induces huge temporal distortions, which manifest as large temporal broadening and amplification. Although a negligible tail could be observed in the pulse for low probe powers [Figs. 4(a)-4(b)], the final pulse shape results completely distorted when using high probe powers [Figs. 4(c)-4(d)]. The largest distortion in this case has been found to be for a frequency detuning of about 20 MHz; however, this worst-case condition depends on the pulse spectral width, which is directly linked to its temporal duration. It is noteworthy the huge amplification and temporal broadening induced when using a probe power of 4 dBm/sideband, resulting in a pulse shape with 30 times higher power and about 4 times longer (i.e. a net energy growth up to 120 times higher than the undistorted pulse energy). Considering that the local Brillouin gain/loss measured by a BOTDA sensor depends on the local energy of the pump pulse [1,6], temporal and amplitude distortions have both a relevant impact on the measured BGS/BLS. The large distortions in the measured BGS and BLS shown in Fig. 1(d) actually originate from the very high local energy transfer from the pulse to the probe occurring at such a high probe power (4

#259757 Received 19 Feb 2016; revised 22 Apr 2016; accepted 24 Apr 2016; published 2 May 2016

dBm). An important consequence of the non-local effects induced in this case is not only linked to the spectral distortions affecting the measurements, but also to the huge temporal distortion of the pump pulse, which obviously has a deleterious effect on the spatial resolution of the system.

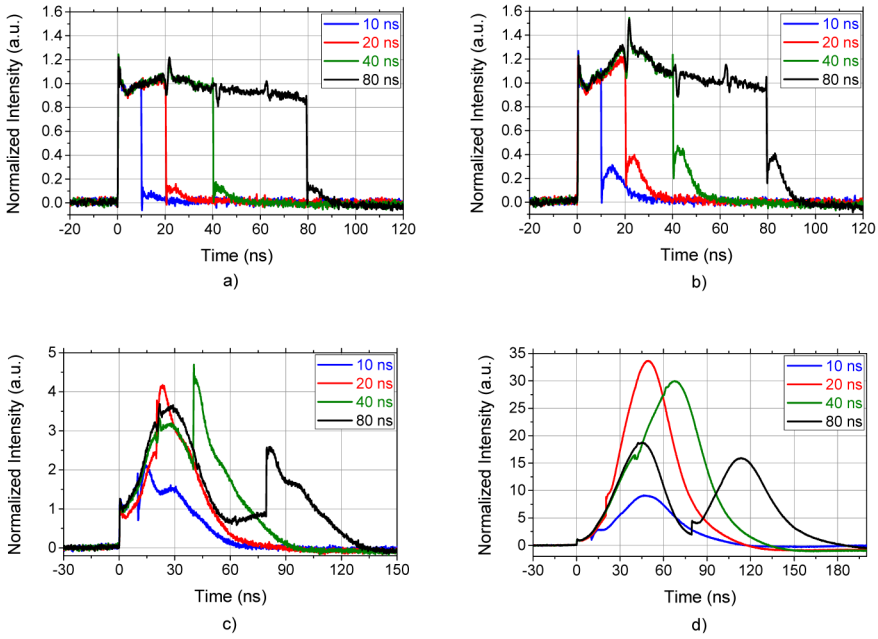

Fig. 5. Temporal distortion of pump pulses having different widths, for a fixed pump-probe frequency detuning equal to ν_B + 20 MHz, when using a probe power of (a) –5 dBm/sideband; (b) –2 dBm/sideband; (c) 1 dBm/sideband; and (d) 4 dBm/sideband.

In addition to the impact of the frequency detuning, the pulse distortion has also been investigated for different pulse widths. Figure 5 shows the pulse temporal shape measured for four different pulse widths, using the same previous four probe powers (ranging from –5 dBm to + 4 dBm). Similarly to the behavior reported in Fig. 4, Fig. 5 also points out that the pulse distortion is actually negligible when operating at a probe power of –5 dBm, or below; however, this rapidly grows when the probe power is increased. In addition, Fig. 5 also indicates that the level of distortion highly depends on the pulse width, which is clearly explained by the differences in the spectral width of the pulse interacting with the two probe sidebands. A visual inspection of the figure actually indicates that the higher amplitude distortion occurs for a 20 ns pulse width; however the real impact on the sensor response depends not only on the amplitude distortion but on the total relative energy growth that pump pulses experience.

In order to fairly quantify the impact that the described distortions have on the sensor response, the total energy contained in the pump pulse has been calculated by simple integration of the temporal shapes above reported. Figure 6 illustrates the integrated energy of the pump pulses measured at the fiber end (50 km) for different pump-probe frequency detuning and several pulse widths. The energy shown in the figure has been normalized by the energy of the undistorted pulses obtained after propagation along the fiber and in absence of Brillouin interaction. As it can be observed, for low probe powers (< –5 dBm) the pulse distortion represents less than 10% of the energy carried by the pulse, independently of the frequency detuning and pulse width. As demonstrated before in Fig. 1, this relative energy variation can be considered low enough to prevent the measured BGS/BLS from being distorted. When the probe power is increased up to –2 dBm, a certain and repeatable

#259757 Received 19 Feb 2016; revised 22 Apr 2016; accepted 24 Apr 2016; published 2 May 2016

distortion pattern appears, inducing a maximum distortion of about 25% at a frequency detuning of ~20 MHz. For higher probe powers, the distortion increases significantly well above the reference pulse energy, reaching levels of up to 170 times larger than the undistorted pulse case. Comparing the results in Figs. 6(c) and 6(d), it is actually possible to observe the highly non-linear growth of the detrimental effects, where the pulse energy distortion grows about ~20 times for a probe power increase of just 3 dB. It is worth noticing that the relative energy distortion here reported clearly highlight the fact that larger relative distortions occur when using shorter pump pulses. This can explained by the broader spectrum characterizing shorter pulses, which turns out to be much more affected by the asymmetric gain-loss process generated by the two probe sidebands when scanning the BGS/BLS. Figure 6 also points out that the shorter the pulse width, the higher the detuning frequency at which these phenomena have a more harmful effect, e.g. being ~20 MHz for a 20 ns pulse width, but ~25 MHz for a 10 ns pulse. Thus, analyzing the entire set of measurements in Fig. 6, it can be generally stated that the worst distortion scenario arises in BOTDA sensors having a spatial resolution of 1-2 m (i.e. using pulses of 10-20 ns), especially when scanning frequency offsets close to ~20-25 MHz.

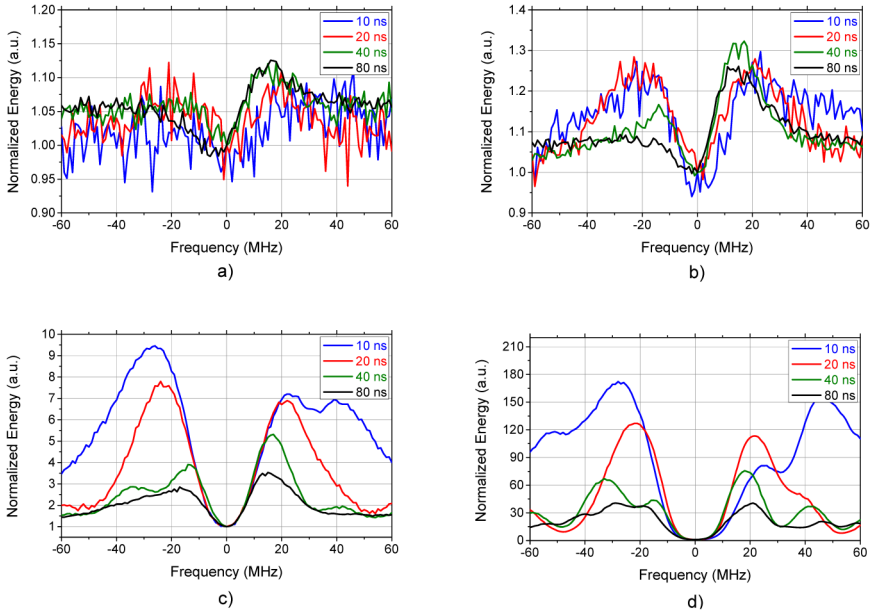

Fig. 6. Total (integrated) pulse energy obtained from the optical pulses measured at the fiber output (after 50 km distance) and normalized by the undistorted pulse energy. Curves are plotted versus the detuning between the pump-probe frequency offset and the dominant BFS of the fiber, for different pulse widths and a using a probe power equal to (a) –5 dBm/sideband; (b) –2 dBm/sideband; (c) 1 dBm/sideband; and (d) 4 dBm/sideband.

It should be mentioned that the leading distortions induced on the pump pulse in both probe power regimes are certainly caused by the SBS interaction between the pump pulse and the probe sidebands (as depicted in Fig. 3). However, it is clear that other non-linearities (such as modulation instability or ASpBS) may arise in the higher probe power regime as a result of the huge variation of the pump pulse energy. It has been checked that these non-linearities have no major effect on the pulse shape, but may eventually lead to a deformation of the measured BOTDA trace.

#259757 Received 19 Feb 2016; revised 22 Apr 2016; accepted 24 Apr 2016; published 2 May 2016

3. Novel BOTDA scanning method

The DSB scheme works perfectly when the gain spectrum is exactly located at the median position between the two sidebands, however, as it has been shown in the previous section, such a scheme still suffers from non-local effects when probe and gain spectra are detuned, even for probe powers far below the ASpBS threshold. Since the asymmetric gain/loss process affecting the pump pulse cumulates along the sensing fiber, severe distortions in the gain/loss BOTDA traces have been obtained, especially at the end of the fiber, where the probe power is the highest. This gives rise to errors in the BFS estimation, and imposes serious limitations to the performance of conventional BOTDA sensors.

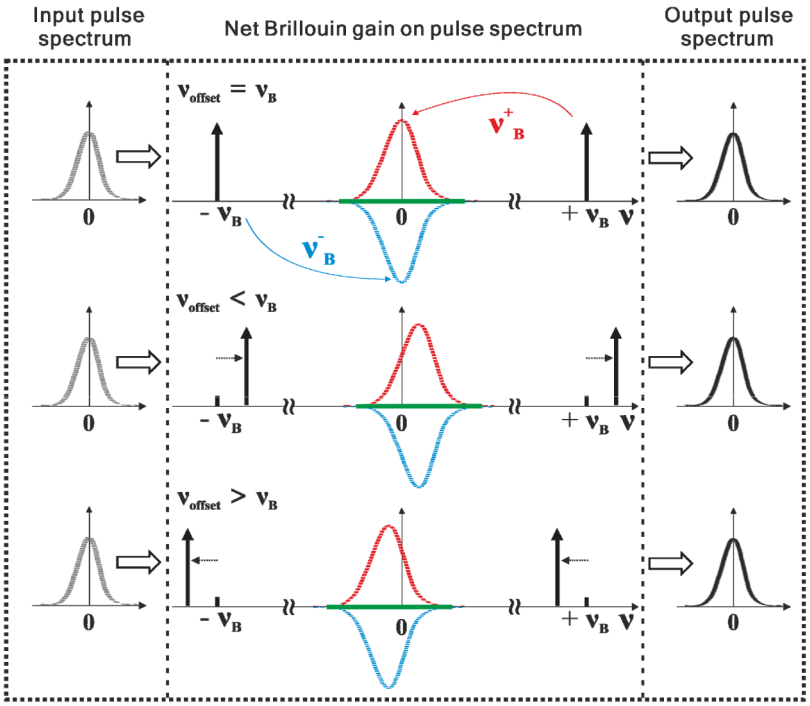

Fig. 7. Net Brillouin gain affecting the pump pulse while scanning the pump-probe frequency offset (ν_{offset}) symmetrically around the pulse spectrum using the proposed scanning method, which keeps a fixed frequency separation between sidebands. Here ν_{offset} refers to the offset between the pump frequency (ν_{pump}) and the probe low sideband frequency ($\nu_{probe\text{-}LSB}$) (i.e. $\nu_{offset} = \nu_{pump} - \nu_{probe\text{-}LSB}$). Grey dotted lines: input pulse spectrum; red dotted lines: Brillouin gain spectrum generated by the upper-frequency probe sideband; blue dotted lines: Brillouin loss spectrum generated by the lower-frequency probe sideband; green solid lines: net Brillouin gain spectrum experienced by the pulse; black solid line: output pulse spectrum after SBS interaction.

In order to overcome those limitations and avoid the distortions affecting the system, a new scanning method is here proposed. In this case, instead of sweeping the two probe sidebands symmetrically away and towards the pulse spectrum as in the conventional case [2,7–9,11], the proposed scheme keeps a fixed frequency separation between the two probe sidebands (equal to twice the dominant BFS of the fiber) while sweeping pump or probe wave frequency to scan the Brillouin gain or loss spectrum, as shown in Fig. 7. Compared to the conventional scanning method (Fig. 2), in the technique proposed here (Fig. 7), the optical pump frequency remains fixed, while the probe sidebands scan towards higher or lower frequencies in unison, keeping a constant separation between them ($2\nu_B$). This way, the gain and loss spectra generated by the two probe sidebands exactly cover the same spectral region and mutually cancel out, regardless of the scanned pump-probe frequency offset (ν_{offset}).

#259757 Received 19 Feb 2016; revised 22 Apr 2016; accepted 24 Apr 2016; published 2 May 2016

Consequently, the pump pulse experiences no spectral distortions during propagation and Brillouin interaction. As demonstrated in the next section, this proposed technique allows the probe power to reach the ultimate limit given by the ASpBS threshold, representing about 12 dB enhancement on probe power when compared to the traditional dual-sideband probe configuration. It must be mentioned that the compensation is fully effective only in the small gain regime – which is confidently the case of BOTDA systems at <5 m spatial resolutions – and with sidebands of equal amplitude.

4. Experimental validation of the proposed method

4.1. Experimental setup

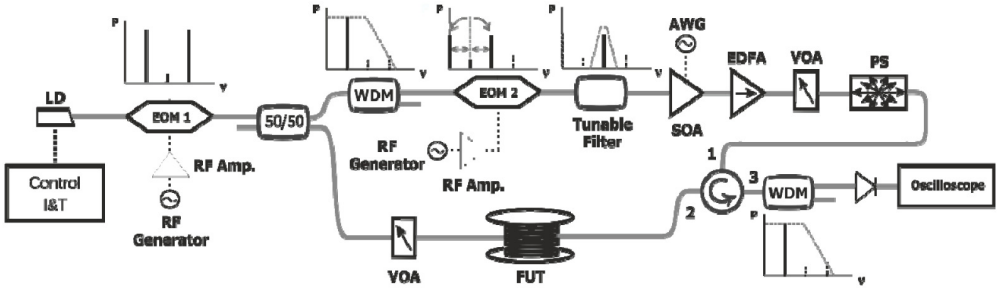

Fig. 8. Experimental setup implemented to validate the proposed scanning technique. LD: laser diode; EOM: electro-optical modulator; WDM: wavelength division multiplexer; AWG: arbitrary waveform generator; SOA: semiconductor optical amplifier; EDFA: erbium doped-fiber amplifier; RF: radio-frequency generator; VOA: variable optical attenuator; PS: polarization scrambler; FUT: fiber under test.

In order to experimentally validate the proposed scanning method, and its ability to measure correctly when using high probe powers, the scheme in Fig. 8 has been implemented. This corresponds to a modified standard BOTDA scheme [7–9,11], where, in this case, the probe wave frequency is fixed while the pump pulse frequency is swept to properly scan the Brillouin gain or loss spectrum. Note that such sweeping implementation is equivalent to the one illustrated in Fig. 7. First, the laser light is modulated using an intensity electro-optic modulator (EOM1), whose modulating frequency is set to match the dominant BFS (ν_B) of the fiber. The generated DSB continuous wave is split into two branches. One of them already constitutes the DSB probe and is directly launched into the sensing fiber, passing through a variable optical attenuator (VOA) that is used to precisely adjust the probe power launched into the fiber. The other branch is used to generate the pump pulse. For this, only one of the two sidebands is selected by a suitable narrowband filter. In this case a dense wavelength-division multiplexer (DWDM) is used to select the low-frequency sideband, which is then amplitude modulated by a second modulator (EOM2) at a frequency difference sweeping around the BFS ($\nu_B \pm \Delta\nu$). This new frequency component, which provides the pump wave, is selected through a narrow tunable filter (~148 pm of bandwidth), wide enough to allow a frequency tuning along the selected spectral span, but narrow enough to filter out all unwanted spectral components. Subsequently, the signal is pulsed through a semiconductor optical amplifier (SOA), then amplified by an erbium doped-fiber amplifier (EDFA) and de-polarized by a polarization scrambler (PS) in order to avoid polarization fading in the measured temporal traces. At the receiver stage, a WDM is used as a narrowband filter to select only one of the probe sidebands, which is then detected by a 125 MHz high-transimpedance photoreceiver (50000 V/A). Note that this high transimpedance gain makes the system thermal noise limited (as demonstrated hereafter) and leads to measurements with optimized electrical SNR [20].

#259757 Received 19 Feb 2016; revised 22 Apr 2016; accepted 24 Apr 2016; published 2 May 2016

4.2. Spectral measurements of the BGS and BLS

In this section the ability of the proposed scanning method to measure correctly even at high probe powers is experimentally verified. It should be noted that all the measurements have been performed for a spatial resolution of 2 m (20 ns pulse width), which actually corresponds to one of the worst conditions as reported in Section 2 and comfortably place the system in the small gain regime. To perform the scan as proposed in the novel method, only the frequency driving EOM2 is swept while the frequency of EOM1 is kept fixed at the dominant BFS over the last kilometers of the fiber. Actually, since the non-local effects under question result from a non-linear SBS interaction, most of the pump pulse distortion cumulates along the last fiber section (equivalent to the non-linear effective length L_{eff}), where the probe power propagating along the fiber is the highest. As a result, in the case of a very long sensing range (longer than α^{-1} ≈20 km), the frequency separation between the two probe sidebands has to be tuned to match the dominant BFS over the last $L_{eff} = \alpha^{-1}$ ≈20 km of fiber. However, as any other non-linear interaction, for shorter sensing fibers (shorter than α^{-1} ≈20 km), the critical interaction length will be reduced accordingly with L_{eff}.

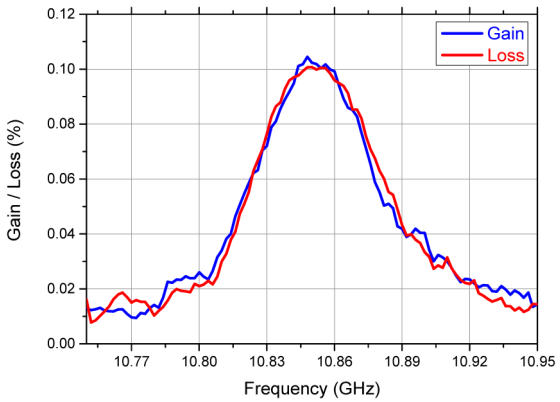

Fig. 9. Measured BGS (blue curve) and BLS (red curve) at the end of a 50 km SMF spool using the proposed method with a probe wave of + 5 dBm/sideband.

Figure 9 shows the BGS (blue curve) and BLS (red curve) measured at the very end of a 50 km uniform SMF spool when a probe wave of 5 dBm/sideband is swept with the proposed method. Interestingly, no distortion is observed in this case. Note that a probe power of 4 dBm in the conventional DBS BOTDA scheme induces huge distortions in both BGS and BLS [see Fig. 1(d)]; however with the proposed scheme these distortions have been reduced to a negligible level even with the use of a slightly higher probe power (5 dBm as employed in Fig. 9). It should be also mentioned that similar spectral shapes have been verified experimentally for lower probe powers, all of them showing the usual bell shape.

To better visualize the correct measurements provided by the method, 3D maps of the measured BGS and BLS are shown in Figs. 10(a)-10(b), respectively. They highlight that no distortions of the measured spectral shape along the entire sensing fiber are observed when using the proposed scheme with a probe power of 5 dBm/sideband. Compared to the conventional scanning method, a clear improvement is here demonstrated. This way the new sweeping method can ensure correct measurement conditions and allows increasing the probe power in at least ~10 dB (from –5 dBm to + 5 dBm), over the standard BOTDA scheme, being ultimately limited by the ASpBS threshold of the fiber (+ 7 dBm) [5], thus representing a 12 dB probe power increase.

It is worth mentioning that due to the increased probe power and the high-transimpedance photodetector used in the measurements shown in Figs. 9-10, an optical attenuator has been placed in this particular measurement at the receiver front-end to avoid saturation of the

#259757 Received 19 Feb 2016; revised 22 Apr 2016; accepted 24 Apr 2016; published 2 May 2016

photodetector. Although no real SNR improvement can be claimed with the use of this attenuator in the system, this technical solution results helpful to demonstrate the significant reduction of the spectral distortions in the BGS/BLS measured when using high probe powers propagating along the sensing fiber. Results certainly validate the proposed scanning method, which best compensates the cumulated gain-loss SBS interaction occurring between the optical signals propagating along the sensing fiber. To complement this demonstration, results in Section 4.3 verify that the proposed method enables the correct detection of a short hot-spot (comparable to the spatial resolution), unlike measurements with the conventional scanning method which are highly affected by the pulse distortions previously described. Furthermore, it should be noted that the mentioned 12 dB increase in the probe power launched into the fiber provides a significant enhancement in the power budget of the system. This can be directly translated into a 12 dB SNR improvement in the measurements obtained by thermal-noise-limited BOTDA sensors. However, if an optical attenuator is needed to avoid saturation and/or other sources of noise dominate, such as shot noise or spontaneous-signal beat noise [19] (resulting when using an EDFA in the probe branch), the SNR improvement provided by the novel scanning method might be reduced. It remains that one of the main benefits of the proposed scanning method is the possibility of reaching longer sensing ranges due to the enhanced probe power that is launched into the sensing fiber, besides the undistorted spectral measurements. The full advantages of the propose scanning methods will be shown in Section 4.4, demonstrating undistorted BGS/BLS measurements along an extended sensing range of 100 km.

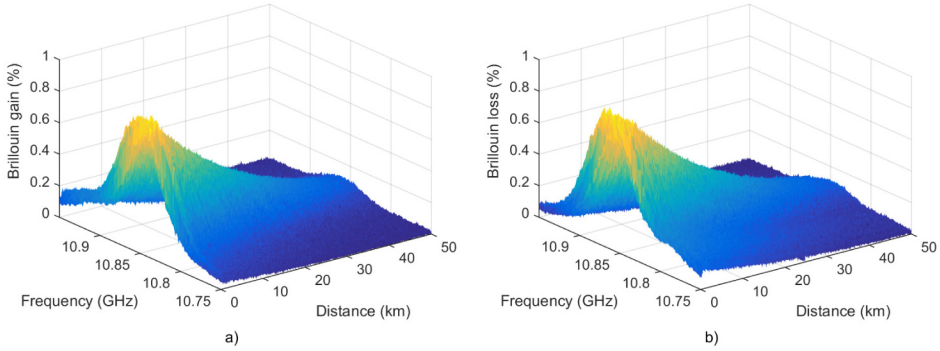

Fig. 10. 3D maps of the measured (a) Brillouin gain spectrum and (b) Brillouin loss spectrum along a 50 km-long sensing fiber, using the proposed scanning method. Compared to standard BOTDA measurements, the spectra in this case are not distorted at any location along the fiber.

4.3. Hot-spot detection

So far the analysis of distortion has been presented for the spectral and temporal shapes measured by the conventional and the proposed method. As reported in Section 2 and in the state-of-the-art [3–5], non-local effects basically impact on the measured traces when long sensing fibers are used, along with high probe powers. The impact is therefore mostly observed over the last kilometers of fiber. If an event, such as a strain or temperature variation, occurs at the end of the sensing fiber, the distortions induced in the conventional BOTDA scheme will completely cover the BGS/BLS spectral shift. For this reason, the measurement of hot-spot placed near the far fiber end becomes essential to validate the proposed scanning method. In order to increase the signal contrast and provide better SNR to the measurements, this test has been carried out using a 25 km-long sensing fiber. It is important to notice that the fiber effective length, determining the ASpBS threshold [5] is only marginally reduced in this case (with respect to the effective length of 50 km, being α^{-1} ≈20 km), representing only a small variation in the conditions when compared to previous results. Nevertheless, to provide a reliable comparison, measurements with the standard

#259757 Received 19 Feb 2016; revised 22 Apr 2016; accepted 24 Apr 2016; published 2 May 2016

BOTDA scheme have been repeated along the 25 km of fiber, and results are compared with the ones obtained with the new proposed method.

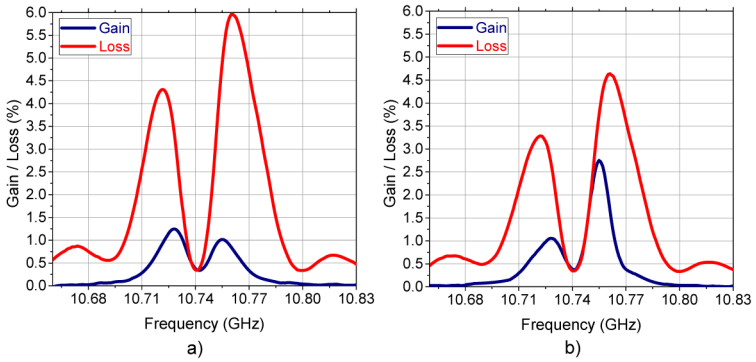

Fig. 11. Brillouin gain and loss spectra measured at the end of a 25 km-long SMF spool where a hot-spot has been applied. (a) Profiles obtained a few meters before the location of the hot-spot. (b) Profiles obtained in the middle of the hot-spot when immersing the fiber in a hot-water bath.

For this test, a 2 meter-long hot-spot has been placed at the end of a 25 km SMF spool, immersing the short fiber section into a hot-water bath at a temperature of ~53 °C, while the room temperature has been measured to be 25 °C. While Fig. 11(a) shows the BGS and BLS measured just before the hot-spot location with the standard BOTDA scheme and a probe power of 4 dBm [same condition as in Fig. 1(d)], Fig. 11(b) shows the measured spectra at the exact position of the hot-spot. The huge distortions observed in this case makes it impossible to retrieve the correct temperature profile. As it can be seen, the 2 m hot-spot placed at the end of the fiber is confirmed to be completely concealed under the huge deformation of the gain and loss curves. Actually, with the level of distortion measured in this case, any fitting algorithm employed to obtain the peak of the BFS will fail to locate the real and proper frequency shift (either outside or at the very location of the hot-spot). For instance, the widely employed parabolic fitting [6] would in this case converge to a polynomial curve adjusted to any of the two strong spectral peaks, leading to a wrong BFS determination.

On the other hand, when the proposed method is used, correct BGS and BLS shapes could be measured, as reported in Figs. 12(a)-12(b). In particular, Fig. 12(a) shows the BGS/BLS measured a few meters before the hot-spot and at its precise location. It is important to mention that similar spectral shapes have been obtained, not only at 4 dBm, as in the case depicted in Figs. 11(a)-11(b) (used here as a reference for comparison), but also using higher probe powers. The particular broadening observed in the BGS/BLS inside the hot-spot shown in Fig. 12(a) is probably due to some non-homogeneity in the heating process implemented to generate the hot-spot on the fiber. Actually, the pump pulses have been monitored at the output of the fiber for several probe frequency detuning to verify any potential impact of residual non-local effects. As shown in the inset on Fig. 12(a), the pulses remain essentially undistorted at the fiber output regardless of the probe frequency detuning, demonstrating negligible levels of non-local effects. It should be noted that the particular case shown in Fig. 12 has been measured with a probe power of 8.4 dBm/sideband, which, to our knowledge, matches the highest probe power reported in a BOTDA sensor to date. This represents a remarkable performance improvement in BOTDA sensing, while ensuring no visual impairment in the measurements. Figure 12(b) shows the retrieved temperature profile around the hot-spot location when using such a high probe power, confirming the correct determination of the applied temperature change.

#259757 Received 19 Feb 2016; revised 22 Apr 2016; accepted 24 Apr 2016; published 2 May 2016

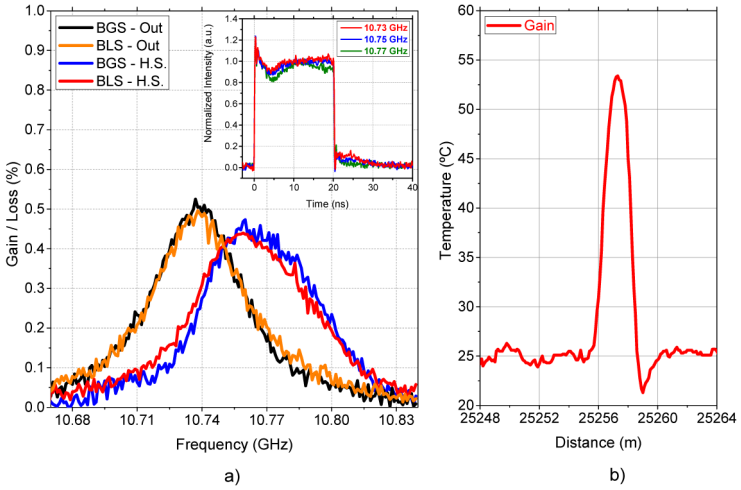

Fig. 12. Detection of a 2 m-long hot-spot with the proposed BOTDA scanning method using a probe power of + 8.4 dBm/sideband. (a) Brillouin gain and loss spectra measured at the end of a 25 km-long SMF spool where the hot-spot has been applied (black and orange lines: a few meters before the hot-spot; red and blue lines: at the precise location of the hot-spot). (a: Inset) Output pulses for several probe frequency detuning. (b) BFS profile translated to absolute temperature around the hot-spot position (profile obtained from the measured BGS).

4.4. Very-long range BOTDA sensor

Making use of the improved operating conditions demonstrated before for the proposed scheme and owing to the increased probe power, measurements along 100 km with 2 m resolution turned possible without the need of additional advanced methods, such as coding techniques [12,13], distributed amplification [14,15], image processing [16,17] or some combinations of them [18,19]. Figure 13(a) shows the BOTDA amplitude trace at the averaged peak gain frequency (pump-probe frequency shift of ~10.856 GHz) along the 100 km fiber span. As it can be observed, the fiber end is perfectly visible, showing a good contrast with the background noise (SNR of ~6 dB at 100 km distance). The decay in the dB scale is perfectly linear, which also ensures that only the linear fiber attenuation is acting on the pump pulse, with negligible levels of pump depletion. The slight disturbance observed at 50 km is due to the fiber pigtails and connectors used to join the two ~50 km SMF spools together. The pump pulse peak power employed in this case is ~14 dBm and the probe wave is ~5 dBm, while each time trace has been averaged 16000 times.

To further verify the performance of the implemented sensor, a 5 meter hot-spot has been placed at the end of the fiber (around 100 km) in a hot-water bath at ~60 °C (the room temperature being about 25 °C). A full frequency sweep is performed to retrieve the BFS change at the hot-spot position; the retrieved temperature profile around the hot-spot is shown in Fig. 13(b). A ~35 °C change over room temperature is verified at the hot-spot location (considering a linear relation temperature-frequency ≈1°C/MHz), which matches the real temperature difference. The sensing uncertainty (estimated as the standard deviation of the repeatability in consecutive measurements) around the hot-spot is 2.4 °C. In addition, the spatial resolution of the system has been verified to be 2 m, which has been determined by analyzing the length of the temperature transient in the detected hot-spot. Moreover, the hot-spot is correctly identified as being ~5 m long.

#259757 Received 19 Feb 2016; revised 22 Apr 2016; accepted 24 Apr 2016; published 2 May 2016

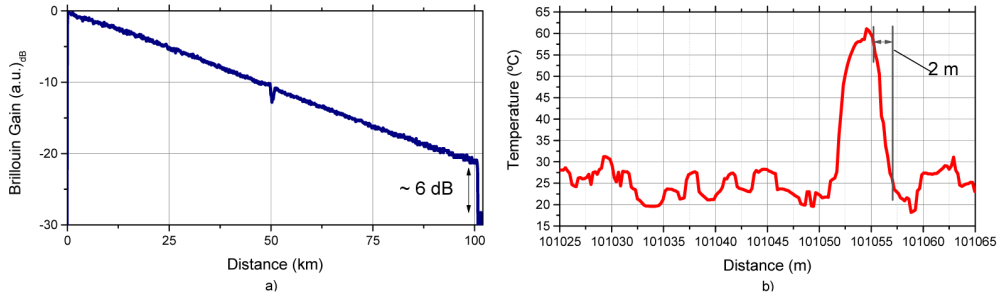

Fig. 13. (a) BOTDA trace represented in logarithmic scale along a 100 km-long sensing fiber, for a pump-probe frequency offset of 10.856 GHz. (b) Retrieved BFS profile translated to the absolute temperature, measured for a ~5-meter hot-spot located around a 100 km distance.

It should be highlighted that this kind of measurements at 100 km with 2 m resolution are basically impossible to perform with conventional DSB setups. These performances can only be reached by using range enhancement techniques such as pump pulse coding [12,13], Raman assistance [14,15], image processing [16,17] or combinations of them [18,19]. This comes from the low SNR resulting from the reduced probe power (<–5 dBm/sideband) required to avoid spectral distortions in the measurements and the large cumulated fiber loss (20 dB for 100 km sensing range) experienced by the probe before reaching the detector. With no preamplification before detection, these features make the BOTDA system to be basically thermal-noise dominated, even when using the raised probe power enabled by the proposed scanning method. This has actually been verified in our setup by measuring the noise standard deviation of the electrical trace measurements (4.37 mV), which is essentially identical to the one measured when no light enters into the photodetector (4.34 mV). Such noise behavior implies that the proposed scanning method provides a figure-of-merit (FoM) [6] enhancement of about one order of magnitude, which follows the ~12 dB SNR improvement accomplished in the implemented BOTDA system. The simplicity of the proposed setup makes these results even more impressive when compared with other studies reaching similar distances.

5. Conclusions

In this paper a thorough analysis of non-local effects impacting on the response of conventional BOTDA sensors based on high-power DSB probe has been presented. Experimental results have verified that, contrary to the common acceptation up to now, non-local effects do appear in conventional dual-sideband BOTDA schemes well below the ASpBS threshold, especially when using long fiber sections showing uniform BFS. The DSB scheme actually works perfectly when the modulation frequency matches the BFS of the fiber, but suffers from non-local effects when the sideband modulation frequency is detuned from the dominant BFS of the fiber. The analysis presented here highlights that the origin of these non-local effects is the uneven spectral compensation of the gain and loss spectra caused by the probe sidebands on the pump pulse spectrum. The pump pulse changes severely its spectral shape when it propagates through a long sensing fiber and interacts with a high-power probe wave. These spectral changes manifest as a shift and an asymmetric energy growth of the pump spectrum depending on the exact detuning from the BFS. Such an asymmetry is directly related to the probe power employed, being larger for higher probe powers. They are also related to the pulse width, so they become more severe when the pulse is shorter (in higher-resolution systems). In addition, measurements have also demonstrated that these spectral distortions turn out to induce strong temporal distortions in the pump pulses at the fiber end, affecting the accuracy and spatial resolution of the measurements. It has been actually verified that the combination of these effects conceals the determination of temperature or strain events in the fiber, especially at the end of long sensing fibers, as the

#259757 Received 19 Feb 2016; revised 22 Apr 2016; accepted 24 Apr 2016; published 2 May 2016

measured gain and loss spectra turns out to be completely distorted, typically showing two side-lobes detuned from the BFS frequency.

To solve these issues, a novel scanning technique for Brillouin optical time-domain analysis has been proposed and validated. The measuring methodology is based on varying the pump-probe modulation structure by just fixing the probe sidebands frequency separation to match twice the dominant Brillouin frequency shift over the last kilometers of fiber ($L_{eff} = \alpha^{-1} \approx 20$ km), and then sweeping the pump pulse frequency. Note that the non-local effects under question would be reduced if the sensing fiber presents several sections with different BFS, since the cumulative effect over the pump pulse is averaged among the different BFS distributions. However, it is usually expected that single fiber spools would show a relatively uniform BFS, making the proposed system helpful for most real-case applications. If the BFS uniformity changes along the fiber, for instance as a result of fiber properties or environmental conditions, the proposed method with a fixed frequency separation between probe sidebands would turn less critical, but would not impair the sensor performance. Only if the BFS distribution along the last kilometers of the fiber presents a considerable and long enough frequency step, the proposed technique could become less effective near the fiber end and even non operative in extreme unlikely situations, but fortunately it will never result in a higher pump pulse distortion when compared to the conventional BOTDA scanning procedure and can be considered as the best case situation in term of cumulated distortion.

This method ensures cancelation of the probe-induced gain and loss spectra over the pump for the complete frequency span analyzed. Experimental results prove that this method enables the probe power to be increased until the onset of ASpBS with no visible distortion on the gain/loss curves, thus providing high robustness against pump depletion and non-local effects. The possibility of raising the probe power is translated into a sensor performance improvement, as the SNR of the measurements can be strongly increased. Of course, matching the proper pump-probe frequency shift of the fiber is critical to ensure correct measurements, but this can be realized by a coarse measurement at large spatial resolution and low probe power. Under these conditions, it is possible to measure a sensing range of 100 km with 2 meter resolution (16000 averages) and 2.4 °C uncertainty, without any extra assistance. Experimental results have demonstrated that, in a thermal-noise-limited BOTDA system, the proposed scheme results in a FoM improvement of about one order of magnitude over the traditional sweeping scheme, directly mapping the 12 dB increase in probe power. This corresponds to a considerable upgrade in the performance of BOTDA sensors, giving the possibility of combining it with other additional techniques, such as Raman assistance, image processing or pulse coding. It can be foreseen that by combining all these techniques, it might be potentially feasible to measure ranges exceeding 150 km of fiber with similar spatial resolution values.

Acknowledgments

This work was supported in part by the European Research Council through the Starting Grant project U-FINE (Grant no. 307441), in part by the Spanish Ministry of Science and Innovation under Project TEC2013-45265-R, and in part by the Comunidad de Madrid under Project SINFOTON-CM:S2013/MIT-2790. Z. Yang acknowledges the China Scholarship Council and BUPT Excellent Ph.D. Students Foundation (CX201431) for supporting his stay at EPFL. The work of S. Martín-López was supported by the Spanish Ministry of Science and Innovation through a “Ramón y Cajal” Contract.

#259757 Received 19 Feb 2016; revised 22 Apr 2016; accepted 24 Apr 2016; published 2 May 2016